Composites Part B 114 (2017) 101–110

Contents lists available at ScienceDirect

Composites Part B

journal homepage: www.elsevier.com/locate/compositesb

Synergistic of ammonium polyphosphate and alumina trihydrate as fire retardants for natural fiber reinforced epoxy composite

P. Khalili [a], K.Y. Tshai [a], D. Hui [b], I. Kong [a, *]

[a] Department of Mechanical, Materials and Manufacturing Engineering, The University of Nottingham, Malaysia Campus, Jalan Broga, 43500, Semenyih, Selangor, Malaysia
[b] Department of Mechanical Engineering, University of New Orleans, Lake Front, New Orleans, Louisiana, LA 70138, USA

ARTICLE INFO

Article history:
Received 7 September 2016
Received in revised form
11 December 2016
Accepted 28 January 2017
Available online 31 January 2017

Keywords:
Hybrid
Polymer-matrix composites (PMCs)
Mechanical properties
Thermal properties
Thermosetting resin

ABSTRACT

Various compositions of epoxy/hardener with flame retardant (FR) as additives were used to produce natural fiber composite through the resin infusion technique. The effects of natural fiber (NF), ammonium polyphosphate (APP), alumina trihydrate (ATH) and ATH/APP hybrid on flammability, thermal and mechanical properties of the composites were investigated. Incorporation of NF into neat epoxy matrix reduced the gross heat of combustion with improved thermal degradation properties. Addition of APP enhanced the flame resistant properties of the composite with a much reduced total flame time and zero drip. The 10 wt·% ATH and 5 wt·% APP hybrid showed the most promising flame retardancy with a self-extinguishing property as well as the lowest gross heat and greatest char residue amongst the various formulations investigated. In general, the formulations containing only ATH couldn't provide the effective flame resistivity as compared to that of the APP-filled composites. The ATH-filled formulations reduced the tensile strength, elongation at break and flexural properties while an increase in the flexural strength of APP-loaded formulations was observed. An increase in moduli of the FR-filled composites was measured as compared to that of the NF/epoxy composite, owing to a more brittle characteristic.

1. Introduction

Over the past decade, the increasing awareness in community health and environment has boosted the utilization of fibres obtained from renewable sources. The usage of natural fiber (NF) composites have been gaining momentum in several applications such as the automotive, furniture and food packaging industries due to their renewability, availability, low density, low cost and appropriate mechanical performances [1–5]. However, the fallbacks such as high flammability behavior of NF, poor compatibility of NF with polymeric matrices of hydrophobic nature, and the high processing temperature of thermoplastic polymers (which adversely affects physio-mechanical performances of NF) [1] broadly limits their wider application, in particularly the venture towards aviation industry which governs by an exhaustive set of stringent regulatory requirements.

Unlike thermoplastics, thermoset resin possess low viscosity prior to crosslink and their fabrication route does not require to be operated at high temperature. The merit of thermosetting polymer provides ease of fabrication for accommodating constituent mixture of NF reinforced composites [6], and it was also found that epoxy resin could exhibit stronger surface interaction than that of the unsaturated polyester. In addition, processing of thermosetting composites can be performed with much lower processing pressure than that of the thermoplastic polymers [7].

Intumescent flame retardants (IFRs) have been widely used to reduce the flammability of polymers, with enhanced properties such as low corrosion and toxicity, reduced smoke emission, increased char formation and anti-dripping flame [8]. IFRs consist of a source of blowing agent, a source of char formation, and an acid source which together capable of generating a foamed char barrier that decreases the transport of fuel and heat into the bulk of the constituents [9–11]. In the event of fire, an intumescent ammonium polyphosphate (APP) agitated by the heat source eliminate ammonia (NH_3) and water while forming ultraphosphate which could act as a protective layer against fire propagation. Alumina trihydrate (ATH) on the other hand undergoes endothermic

* Corresponding author. Department of Mechanical, Materials and Manufacturing Engineering, The University of Nottingham, Malaysia Campus, Jalan Broga, 43500, Semenyih, Selangor, Malaysia.
E-mail address: ing.kong@nottingham.edu.my (I. Kong).

http://dx.doi.org/10.1016/j.compositesb.2017.01.049
1359-8368/

dehydration upon fire, releasing water vapor which function as diluent for the combustible gases with concurrent formation of a thermally stable ceramic alumina (Al_2O_3) that serve as an insulating layer against heat and mass transfer [12,13]. The chemical structures of APP and ATH are shown in Fig. 1. However, increasing the concentration of FRs in a polymeric formulation often associated with reduction in mechanical performances and inevitably increased material cost, thus the smallest effective FR loading, which could be up to 20 wt·%, is generally desirable [14]. From the manufacturers' perspective, it is crucial to derive the optimum amount of IFRs to meet the demand for fire retardant system.

Castronvinci et al. [15] investigated the effects of APP/ATH hybrid on fire retardancy of styrene butadiene rubber (SBR) block copolymer noticed clear interactions between APP and ATH as a FR system. The chemical reactions took place over a varying range of temperatures. The chemical reaction first occurred between APP (NH_4PO_3) and hydroxyl groups (−OH) of ATH at a temperature lower than 400 °C (Fig. 2). This resulted in the formation of aluminum phosphate with generation of water and ammonia (NH_3) out of ammonium salt (NH_4). These reactions kept repeating until aluminum metaphosphate ($[Al(PO_3)_3]_n$) was formed.

At higher temperature, further reactions took place forming aluminum orthophosphate ($AlPO_4$) from the long chain polyphosphate as well as releasing ammonia and water (Fig. 3).

The combined effect of APP/ATH contributed to an improved fire extinguishing behavior due to a number of factors. Firstly, the generation of aluminum phosphate prevents the evaporation of phosphorous volatility. Secondly, the basicity of ATH that furnish protons exchange and an easier evolution of water and ammonia gas. Thirdly, the crystalline form of Al-P-O alters the glassy ultraphosphate structure by which gases can readily escape the solid surface.

Introduction of NF into neat polymers reduced the heat release and enhanced flame retardant performances relative to those of the pure matrices [16–18], and incorporation of small loading level of FR could further reduce the flammability behavior of biocomposite at the cost of a slight drop in mechanical properties. Few reports

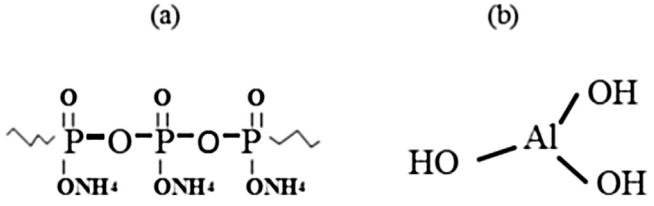

Fig. 1. The chemical structures of (a) APP and (b) ATH.

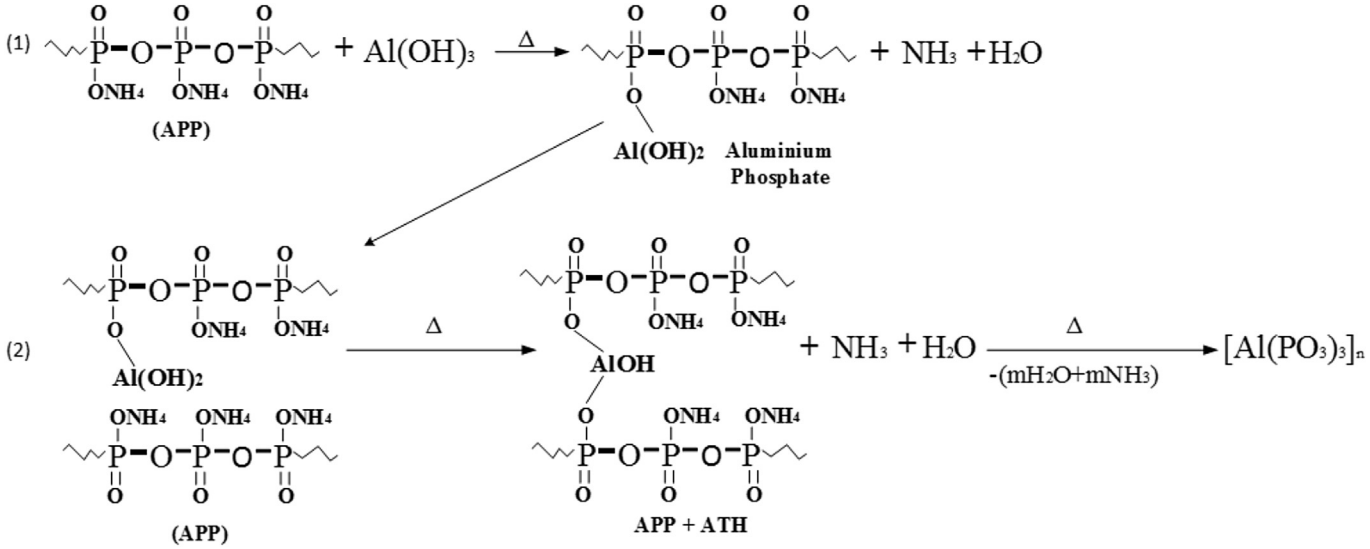

Fig. 2. Reactions between ATH and APP.

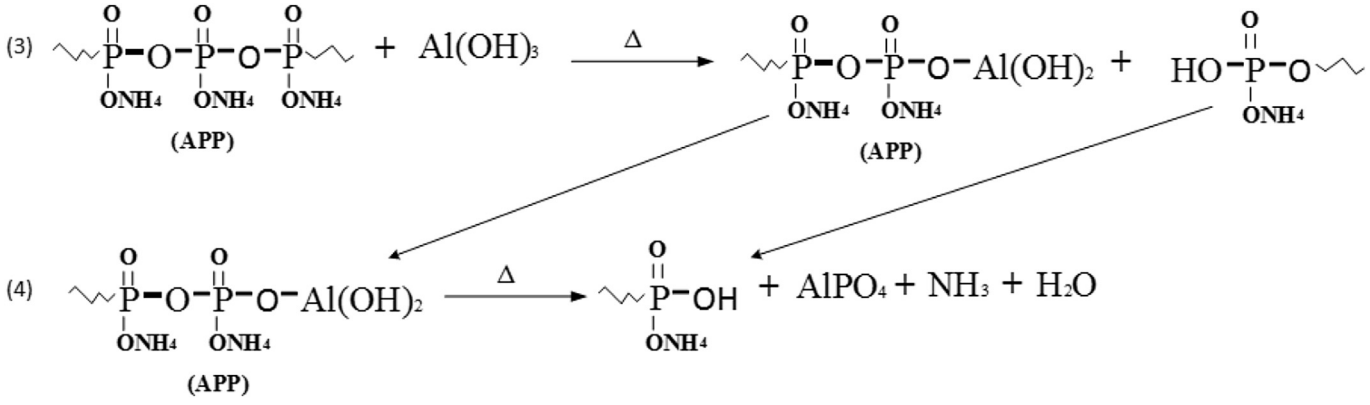

Fig. 3. Reactions between ATH and APP at elevated temperatures.

[19–21] have been published on the enhancement of flammability, thermal stability and mechanical properties of NF based composites using FRs and no previous studies were conducted to investigate the effect FRs on the fire resistant of the palm empty fruit bunch (EFB) fiber reinforced epoxy based composite. This work aimed to study the combined effects of APP, ATH and EFB fiber on the flame resistivity and mechanical performance of the resulting composite by means of a series of characterizations to obtain an optimized composition of the constituent loadings.

2. Methodology

2.1. Materials

Alumina trihydrate (ATH) with median particle size of 1 μm in diameter was purchased from J. M. Huber Corporation (Malaysia); ammonium polyphosphate (APP) powder of grade Exolit AP 422 (degree of polymerization > 1000) was provided by Clariant (Singapore) Pte Ltd; an ambient cure two part epoxide resin system Ultimeg 2020 was purchased from AEV Asia Sdn. Bhd. (Malaysia). The viscosity of mixture of epoxy and hardener at 25 °C was measured 0.2–0.6 N s/m^2; pulverized palm EFB fiber was purchased from Szetech Engineering Sdn Bhd. The EFB fiber had an average length in the range of 10–20 mm and bundle diameter 100–200 μm; a water based formaldehyde-free cross-linked acrylate binding agent, Acrodur DS 3530 was supplied by BASF Malaysia Sdn. Bhd.

2.2. Composite fabrication

2.2.1. Fiber mat

Randomly-orientated EFB fibers were dispersed in a water-binder suspension of 10:1 (v/v) ratio to form a mat in a customized sieve (180 mm × 320 mm). Fiber length of 1 cm was chosen to avoid fiber entanglement and to encourage even distribution of fiber during mat fabrication [22]. The sieve was then taken out where draining of water took place. The fiber mat was then flipped upside down onto pieces of dry cloth, and another layer of dry cloth was placed on top of the fiber mat to absorb residual water from both sides. The bonded mat was shifted to metal plates with blotting papers on top and bottom of the mat. A load of 15 kg (equal to 2.6 kPa) was then applied on top of the fiber mat for 10 min to press out the remaining water and to produce a mat with an even thickness of 1 mm. Fully soaked blotting papers were replaced with new ones and pressed with the same weight until the mat was visibly dried. The dried fiber mat was subsequently placed within a convection oven maintained at 100 °C for 4 h with an applied top loading of 4 kg while measurements were taken to ensure the fiber mat showed no further weight loss due to moisture evaporation. The dried fiber mat was further kept dry within the oven at a lower temperature of 70 °C for 24 h until resin infusion was to be carried out. The fiber mat was dried under selected temperature to ensure that the structure and properties were not damaged by the extreme temperature.

2.2.2. Resin infusion

A summary of the composite fabrication process is outlined. In the first stage, a PVC plate was sprayed with silicone release agent. Then gum tape was applied around the perimeter of the mold and the EFB fiber mat was placed into the mold. A layer of peel-ply was positioned on the EFB mat. This was followed by an infusion mesh that helped the resin to flow and distribute through the mold. Subsequently an infusion spiral and resin feed silicone connector was fitted to the vacuum system. Then vacuum line silicon connector was positioned and the bagging film was stuck to the gum tape. Resin feed hose was connected to the bag and another PVC hose was firmly connected to the bag through vacuum line. An infusion line clamp was used to close the resin feed line and, as a result, evacuating air from the vacuum system. At the stage where full vacuum was achieved, the sealed bag was left for 15 min to ensure there isn't any leakage. Prior to resin infusion, FRs were added into the epoxy resin and approximately 15 min of ultrasonication was applied using a UP400S Ultrasonicator from Hielscher Ultrasonics GmbH at a frequency of 24 kHz and 50% amplitude until a homogeneous dispersion was achieved. Hardener was added into the sonicated mixture at a weight ratio of 5:1 (epoxy:hardener). The mixture was then infused throughout the fiber mat in the mold. The curing took place under room temperature for 24 h at atmosphere temperature (Fig. 4). The combination of neat epoxy and EFB fiber, as control sample, was also prepared for comparison purpose. The formulations of the constituents and their abbreviations are depicted in Table 1.

2.3. Characterization

2.3.1. Vertical Bunsen burner test

Bunsen burner test was carried out in accordance with Federal Aviation Regulation (FAR) part 25.853-b (equivalent to ASTM F 501, Daimler-Benz Aerospace ATS 1000.001, Douglas DMS 1511, Boeing BSS 7230 F2, British Aerospace BACM 155A and Airbus ATS 1000.001) to determine flammability characteristic of the

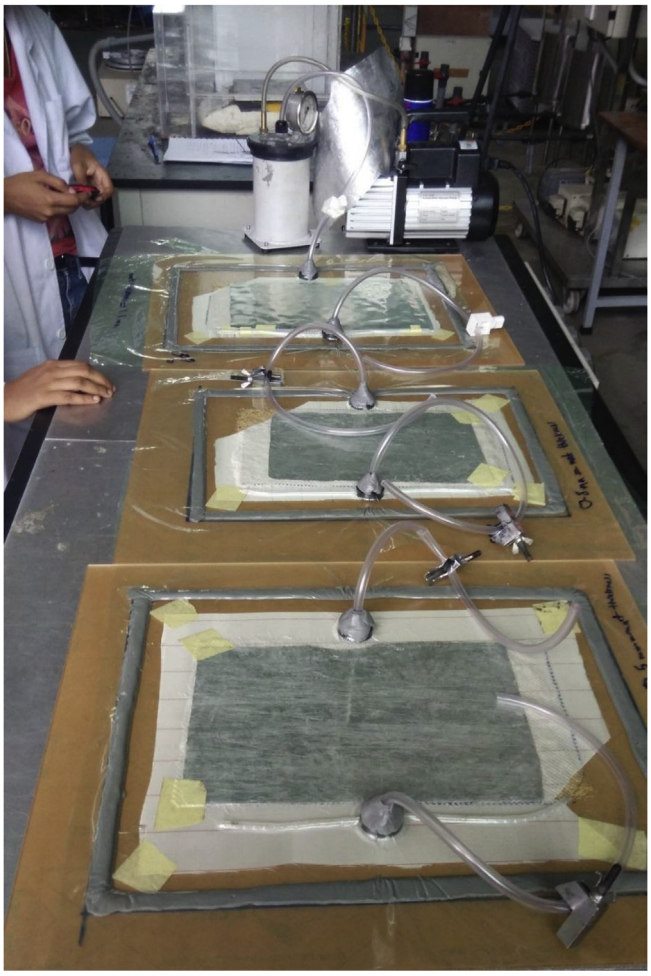

Fig. 4. The composites left to cure after the resin infusion process.

Table 1
Formulations of constituents.

Sample name	ATH (wt·%)	APP (wt·%)	EFB fiber (wt·%)	Epoxy (wt·%)
E100	–	–	–	100
E82F18 (Control)	–	–	18	82
CATH5	5	–	18	77
CATH10	10	–	18	72
CATH15	15	–	18	67
CAPP5	–	5	18	77
CAPP10	–	10	18	72
CAPP15	–	15	18	67
CATH5APP10	5	10	18	67
CATH10APP5	10	5	18	67

materials. Three specimens measuring 152.5 × 37.5 × 2 mm^3, equivalent to half of the standard FAR specified dimension was tested for each formulation. The specimens were held vertically via a lab stand and flamed for 12 s using methane fuel supplied by Bunsen burner placed directly under the specimen. The total flame time, mass loss percentage and drip flame time were measured to analyze the flammability properties. In order to meet the FAR requirements, the average flame time, drip flame time and burn length are required to be below 15 s, 3 s and 152 mm.

2.3.2. Bomb calorimeter

Bomb calorimeter was used to validate the heat capacity of compounds prompted by FRs filled natural fiber reinforced composites. Gross heat of combustion was measured by PARR 6100 bomb calorimeter according to ASTM D-240 standard. 1 mL of water was contained in the metal bucket where the specimen was placed and gradually bomb charged with O_2 to 30 atm (3 MPa) at ambient temperature. Sample weight of 0.8–1 g was placed in a cylindrical crucible and the specimen was linked to the fused wire for combustion to occur. At least two samples from each formulation were tested and the average measurements were computed. The results attained from the bomb calorimeter were repeatable to approximately ±99.85%.

2.3.3. Thermal stability (TGA)

The thermal stability was evaluated on a TGA 1 STARe system (Mettler Toledo) Q500 instrument. Specimen of approximately 10–15 mg in weight was placed in an open alumina pan under nitrogen flow rate of 50 ml/min and heated from ambient (30 °C) to 600 °C at a heating rate of 20 °C/min. The char residual and thermal degradation temperature (T_d) were calculated.

2.3.4. Tensile testing

Rectangular specimens of 120 × 20 × 2 mm^3 were tested with the aid of a Llyod Instruments LR50k Testing Machine in accordance to ASTM D3039 at a crosshead speed of 2 mm/min and the load-cell of 5 kN was used. Five specimens of each formulation were tested using a gauge length 60 mm and the mean value was recorded.

2.3.5. Flexural testing

Rectangular specimens of 100 × 20 × 2 mm^3 were tested using a Llyod Instruments LR50k Testing Machine in a three point bending mode with a span length of 60 mm in accordance to ASTM D790. Crosshead speed of 5 mm/min and load-cell of 5 kN were used. Five specimens of each composition were tested and the mean values were used to analyze the flexural properties of the various formulations.

2.3.6. Scanning electron microscopy (SEM)

SEM was carried out on FEI Quanta 400F FESEM microscope at the increasing voltage of 20 kV. The SEM micrograph of the composites' fractured surfaces was used to observe the adhesion, dispersion and load transfer between the fiber, FRs and epoxy.

3. Results and discussion

3.1. Flammability

The control sample (E82F18) was fabricated to provide proper comparisons with FR-loaded formulations. The results recorded in terms of drip flame time, total flame time and mass loss (wt·%) are shown in Fig. 5. Incorporation of ATH into EFB fiber reinforced epoxy composite did not reduce the burning resistivity, as compared to that of the control sample (E82F18), in terms of drip flame time and total flame time. All of the ATH-filled composites burned intensely and brightly with severe dripping. Adding more ATH fillers reduced the total flame time, with increasing of drip flame time. With increasing loading of APP, the total flame time slightly reduced. The lower total flame time and no dripping phenomenon were detected for all APP-filled composites relative to those of other formulations. This is probably due to the degradation of APP that leads to the formation of a strong char barrier which limits heat and mass transfer, with release of ammonia and water which dilutes the gaseous phase. Suardana and Lim [23] found that degradation of APP generates phosphoric acid which could interacts with the hydroxyl group of natural fiber to form phosphorous esters. This ester acts as catalyst for dehydration of fibers, leading to the formation of a carbonaceous structure with reduction of vapor phase composition and released energy. CAPP10 showed 5% lesser mass loss than that of CAPP5 and displayed 12% reduction in the mass loss compared to that of CAPP15. Also, similar optimum concentration of APP particle in the range of 3–20 wt·% was achieved at 10–12 wt·% by Castrovinci et al. [15]. The flame resistivity of APP at higher loading (>10 wt·%) tends to be lower, implying that APP can affect either positively or negatively depending on the optimum loading.

APP is much more effective than ATH in flame resisting composites. It was observed that [15] inclusion of 60 wt·% ATH was required to achieve similar flame resistivity effect attained with 10–12 wt·% APP. However, composites with higher concentration of ATH were prone to significant drop in mechanical properties.

Exceptionally, when 10 wt·% APP and 5 wt·% ATH were introduced into the EFB reinforced epoxy composite, a synergistic effect took place that created self-extinguishing properties upon the removal of Bunsen burner. However, formulation with 10 wt·% ATH and 5 wt·% APP couldn't establish self-extinguishing behavior but zero drip flame was still maintained. The synergistic effect of the combined APP and ATH was discussed earlier in the introduction section.

3.2. Analysis of residual char

Fig. 6 shows the structure of composites containing APP and APP/ATH upon completion of the flammability tests. The composites with ATH-based additive burned more vigorously than those loaded with APP, and no mass residue was left in the clamp of lab stand. All the burned parts of ATH loaded composites fell down on the tray placed and ATH filled composites couldn't retain the structure. This is owing to the greater flame resistivity of APP than that of ATH as this filler could not adequately confine the pyrolysis process and volatile gases liberation during the fire, expediting the combustion progression and increasingly deteriorating the structure.

As seen in Fig. 6, the bulk structure was maintained in APP filled composites. The hybrid of ATH and APP exhibited its synergistic effect where inclusion of 5 wt·% APP and 10 wt·% ATH (in

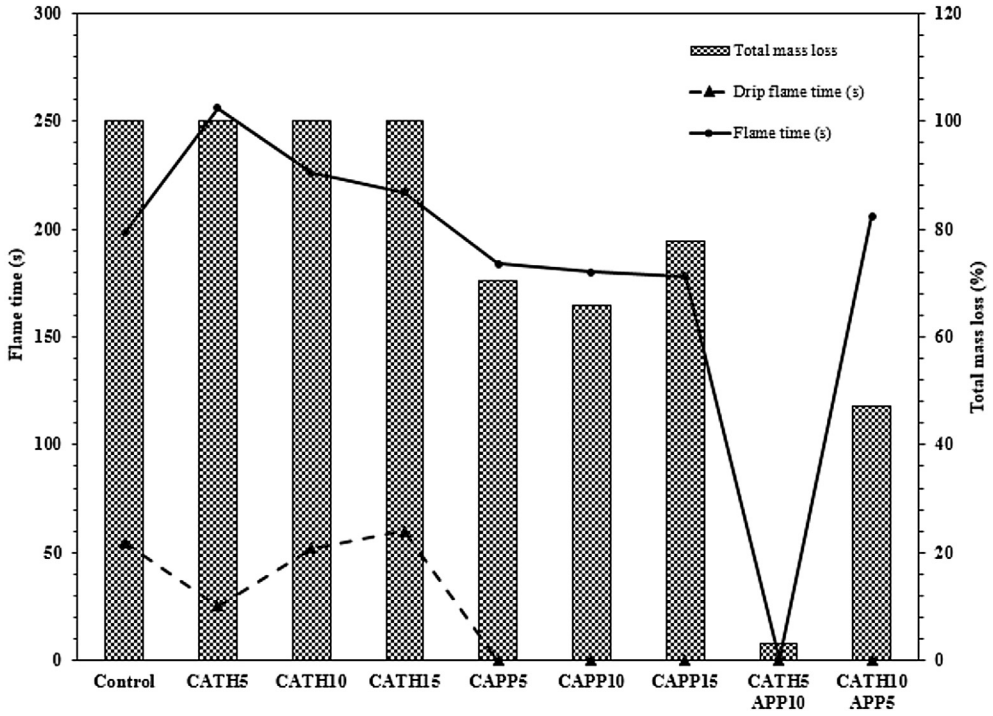

Fig. 5. The results of vertical Bunsen burner testing for the control sample and the composites filled with FR.

CATH10APP5 formulation) could prevent the drip of flame. When the replacement was changed to the optimum value of 10 wt·% APP and 5 wt·% ATH (in CATH5APP10 formulation), self-extinguishing properties were observed. This composite burned for < 1s upon removal of Bunsen burner after 12 s of continuous exposure to direct flame and created zero drip flame and burn length of less than 1 cm with merely 3% mass loss.

It would be noteworthy to add that pieces of control sample broke off on the burning edge and subsequently dropped while this phenomenon didn't occur for all the composites containing ATH and APP. This shows the effectiveness of APP and the hybrid of APP/ATH on the NF-reinforced epoxy composites.

3.3. Bomb calorimetry study

The bomb calorimetry testing was used to investigate the heat of combustion of the reaction between the composites and oxygen measured based on the changes in temperature of the water. The gross heat (GH) of combustion evaluated by the bomb calorimetry exhibits the combustibility of the composites. Pure epoxy burned wildly when subjected to combustion, with GH of 35.36 MJ/kg, as shown in Table 2. When EFB fiber was introduced into pure epoxy, a large drop in the GH, 11.02% was observed, which is in agreement with those reported in literature [24]. This can be attributed to lesser gross heat of combustion of EFB fibre than that of the neat epoxy.

The incorporation of ATH or APP into epoxy/EFB fiber led to a reduction in GH. APP demonstrated 3.83% reduction in combustion performance of EFB fiber reinforced epoxy composite at low loading (5 wt·%). Upon the addition of 10 wt·% APP, the GH reduced by 6.91% relative to that of the control sample, which is due to lesser heat of combustion of APP particles. APP generates water and ammonia which mitigates the gaseous state. The flame resistant effect for the composites containing APP reached optimum when 10 wt·% APP was added. The same trend of heat release was recorded [15] when 3 to 20 wt·% of APP was incorporated into polymeric formulations, the greatest flame resistivity was observed in formulations containing 10–12 wt·% APP. This signifies the dual flame retardancy impact of APP on polymeric composite that can be either enhancing or dropping depending on the amount of APP.

The incremental introduction of ATH could further slowdown the heat release of combustion. This FR decomposes during combustion, generating water in the vapor state through pyrolysis and alumina (Al_2O_3). The water leads to an endothermic process, which removes the heat from the underlying layers. The Al_2O_3 layer also acts as a shielding barrier against the transfer of heat and mass.

The hybrid APP and ATH tested (CATH5APP10 and CATH10APP5) recorded the lowest GH, 13.9% drop relative to that of the control sample, implying their synergetic effect and the optimal weight ratio as evaluated in this work, in agreement with results from Bunsen burner analysis. The hybrid of APP and ATH resulted in a thermally stable surface shielding with aluminum orthophosphate Al-P-O_4 crystalline compounds rather than the ultraphosphate, and more complete elimination of ammonia and water which enhance the thermal surface shielding of composites.

3.4. Thermal properties

The TGA testing was conducted in nitrogen atmosphere, as illustrated in Table 3 and Fig. 7. For the pure fiber, the initial thermal degradation (50–130 °C) occurred with a slight mass loss which can be ascribed to the evaporation of water content. A subsequent sharp drop took place in the temperature range 220–315 °C, mainly due to the weight loss of hemicellulose followed by the pyrolysis of cellulose at temperature regions 315–400 °C. The degradation of lignin took place over a large temperature range ~160–600 °C. The low molecular weight protolignin degrades first but at a slower rate than other constituents [25,26]. The poor linkage was ruined between 170 and 230 °C whereas the debonding of stronger structures in aromatic rings occurred at elevated temperature. It's worth noting that lignin content and thermal stability possess an inverse relationship, i.e. higher concentration of lignin increases the

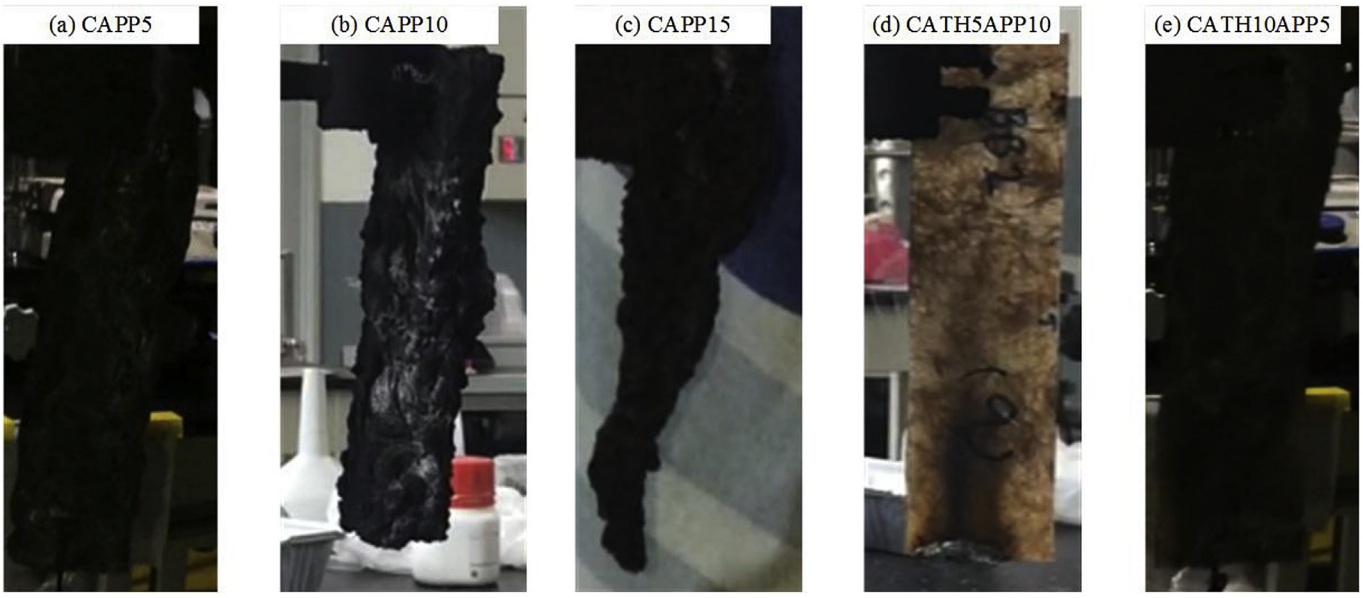

Fig. 6. Digital photos of burnt samples of (a) CAPP5, (b) CAPP10, (c) CAPP15, (d) CATH5APP10 and (e) CATH10APP5 composites after vertical Bunsen burner experiment.

Table 2
The gross heat of combustion of E100, control and composites filled with FR from bomb calorimeter experiment.

Formulations	Gross Heat (MJ/kg)	Decrement of GH from the control composite (%)
E100	35.36	11.02
Control	31.85	0.00
CATH5	30.55	−4.08
CATH10	30.00	−5.81
CATH15	28.56	−10.34
CAPP5	30.63	−3.83
CAPP10	29.65	−6.91
CAPP15	31.50	−1.09
CATH5APP10	27.41	−13.95
CATH10APP5	27.40	−13.96

Table 3
TGA results of the EFB fibre, control and formulations loaded with APP and ATH.

Formulations	Char Residual at $T_{600°C}$ (wt·%)	T_d (°C) at 50 wt·% mass loss
EFB fiber	30.72	346.8
E100	13.59	380.0
Control	15.56	385.8
CATH5	20.47	383.3
CATH10	21.20	388.5
CATH15	22.16	389.3
CAPP5	21.41	376.7
CAPP10	22.20	358.0
CAPP15	19.50	376.0
CATH5APP10	29.18	368.2
CATH10APP5	24.43	368.4

thermal stability. The solid charred residual up to 400 °C can be attributed to the pyrolysis of lignin and the cellulose.

The composites containing FR started to break down at approximately 300 °C owing to the thermal degradation of epoxy resin. The major weight loss started at approximately 315 °C and sustained for at least another 100 °C. Incorporation of APP was observed to enhance the char residue content, where a hybrid of 10 wt·% APP and 5 wt·% ATH resulted in the highest recording. This increment can be ascribed to the degradation of APP and ATH that leads to the formation of aluminum orthophosphate and aluminum metaphosphate. However, APP addition to the composites reduced the onset of thermal degradation temperature, T_d since APP releases water upon thermal degradation [27,28] and contributed to a premature degradation of epoxy as a result of hot water hydrolysis. Besides, the second reason of reduced thermal degradation temperature is owing to the presence of phosphate groups, which decomposes earlier to generate thermal char [29,30]. Similar fashion of lower T_d was observed when APP was incorporated with epoxy [31], and into PP [32]. The same trend of higher post combustion mass residual with increasing APP loading was reported in the work of Dorez et al. and Wen et al. [1,8], respectively. In general, the thermal decomposition mechanism of NF filled composites can be categorized into two stages: the first stage corresponds to the fiber phosphorylation and its degradation at low temperature [33,34] while the subsequent stage corresponds to the matrix decomposition. APP interacts with both the polymer matrix and natural fiber, and mainly fiber lignin content [35], leading to the formation of shielding charred barrier for mass and heat transfer. The existence of phosphate groups in the structure of APP relatively lowers the thermal decomposition temperature and subsequently forms a protective charred layer which retards the epoxy degradation [29,30,36].

With increased loading of ATH, the mass residue and thermal stability improved when heated, which can be attributed to its decomposition into water vapor due to endothermic reaction and conversion to the thermally stable aluminum oxide [$2Al(OH)_3 \rightarrow Al_2O_3 + 3H_2O$] that demonstrates a very high melting temperature of 2054 °C [37].

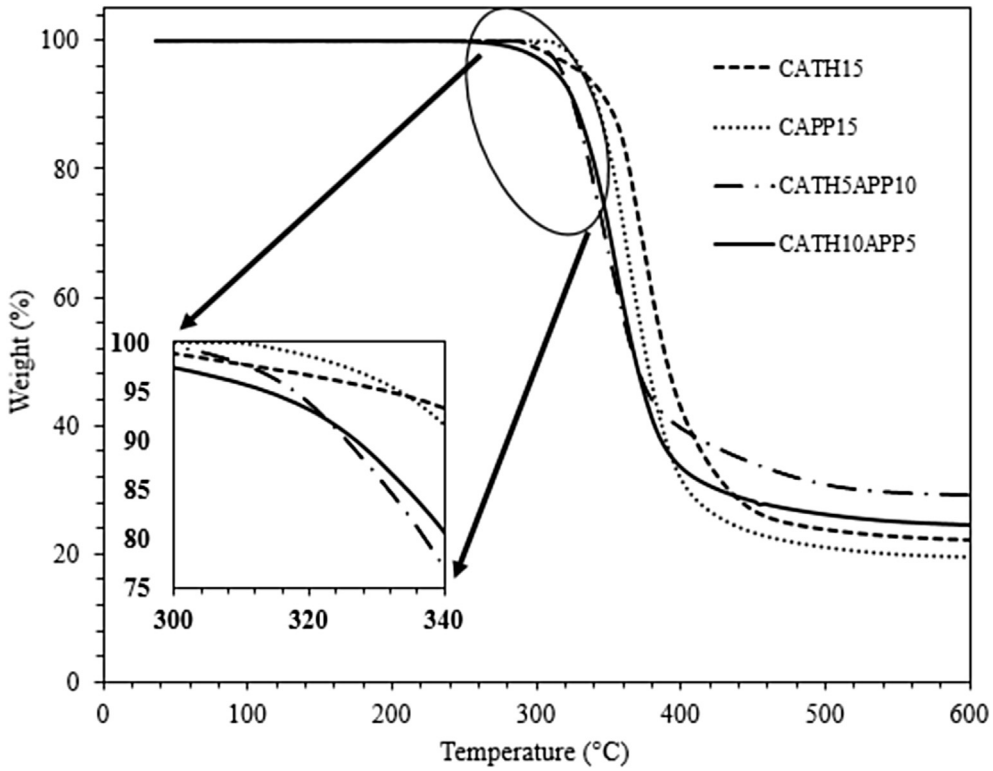

Fig. 7. The degradation behaviors of the selected formulations containing APP and ATH.

Synergistic effect was detected when the combined ATH/APP was used, where enhanced mass residue was recorded with approximately 87.53% and 57% for CATH5APP10 and CATH10APP5 relative to that of the control sample, respectively. The T_d, which was computed at 50 wt·% mass loss, wasn't affected due to the presence of APP in the mixtures. The same synergetic effect was observed in the Bunsen burner and bomb calorimetry analyses.

3.5. Tensile properties

The tensile strength, strain and modulus of composites containing FR and the control sample (E82F18) are shown in Fig. 8. Intumescent flame retardants (IFR) considerably influence the mechanical properties of polymeric composites. The incorporation of IFR significantly reduced the tensile strength of the composite relative to that of the control sample. FRs acted as a nucleating agent, reducing tensile strength, and decreasing elongation at break except those with lower FR loadings. It has been previously shown that APP develops moisture absorption characteristic in wood reinforced composites, resulting in reduced mechanical properties [38]. Incorporation of APP has been associated with decreased tensile strength of formulations in numerous work [8,9,34,39] as well as reduction in the elongation at break [34,39], which was attributed to the poor compatibility between APP and polymer matrices. In the current work, the formulation with 10 wt·% APP loading showed higher tensile strength than that of 5 and 15 wt·% APP filled composites. The control sample demonstrated an approximately 13% greater tensile strength than that of the formulation with 10 wt·% APP. Compared to that of the control sample, the elastic modulus of APP-based formulations was enhanced, generally owing to the reduction in elongation to break and an increasing brittleness of the composites.

The average tensile stress of composites with low loading of ATH, i.e. 5 wt·% concentration, was 19.1% lower than that of the control sample. The Young's modulus of the composites with 10 wt·% and 15 wt·% ATH loadings increased relative to that of the control sample. Similar fashion was observed in the tensile properties of ATH-filled thermoset polymer by Petersen et al. [40]. Incorporation of FRs generally provides higher modulus than that of the control sample. Ramazani et al. [41] observed that the modulus was higher or slightly lesser with increasing ATH loading in the composites than that of the control sample. For the hybrid composites, the tensile strength and strain reduced while the Young's modulus increased relative to that of the control sample.

3.6. Flexural properties

Fig. 9 shows the flexural properties of the formulations. APP-filled composites were observed to possess greater flexural strength than that of the control. The flexural strength was the highest at 5 wt·% APP loading, with ~34% increment as compared to that of the control, followed by 10 wt·% APP and 15 wt·% APP. The decline in flexural strain and strength with increasing FR loading was caused by the poor interfacial adhesion between the FRs and epoxy, which became increasingly significant at higher FR concentration.

Lim et al. [36] attained similar trend in which increasing APP loading resulted in a drop of the flexural performance of glass fiber/epoxy APP loaded composite, and flexural strengths of APP filled composites were all higher than that of the control sample. The control sample showed greater flexural strength and strain than those of the ATH-filled composites and increasing addition of ATH loading decreased the flexural properties of composites. The flexural strength of CATH10APP5 was slightly lesser than the strength of CAPP5 and the flexural strength of CATH5APP10 further dropped relative to that of CATH10APP5. The strain values of the hybrid composites were lesser than that of CAPP5.

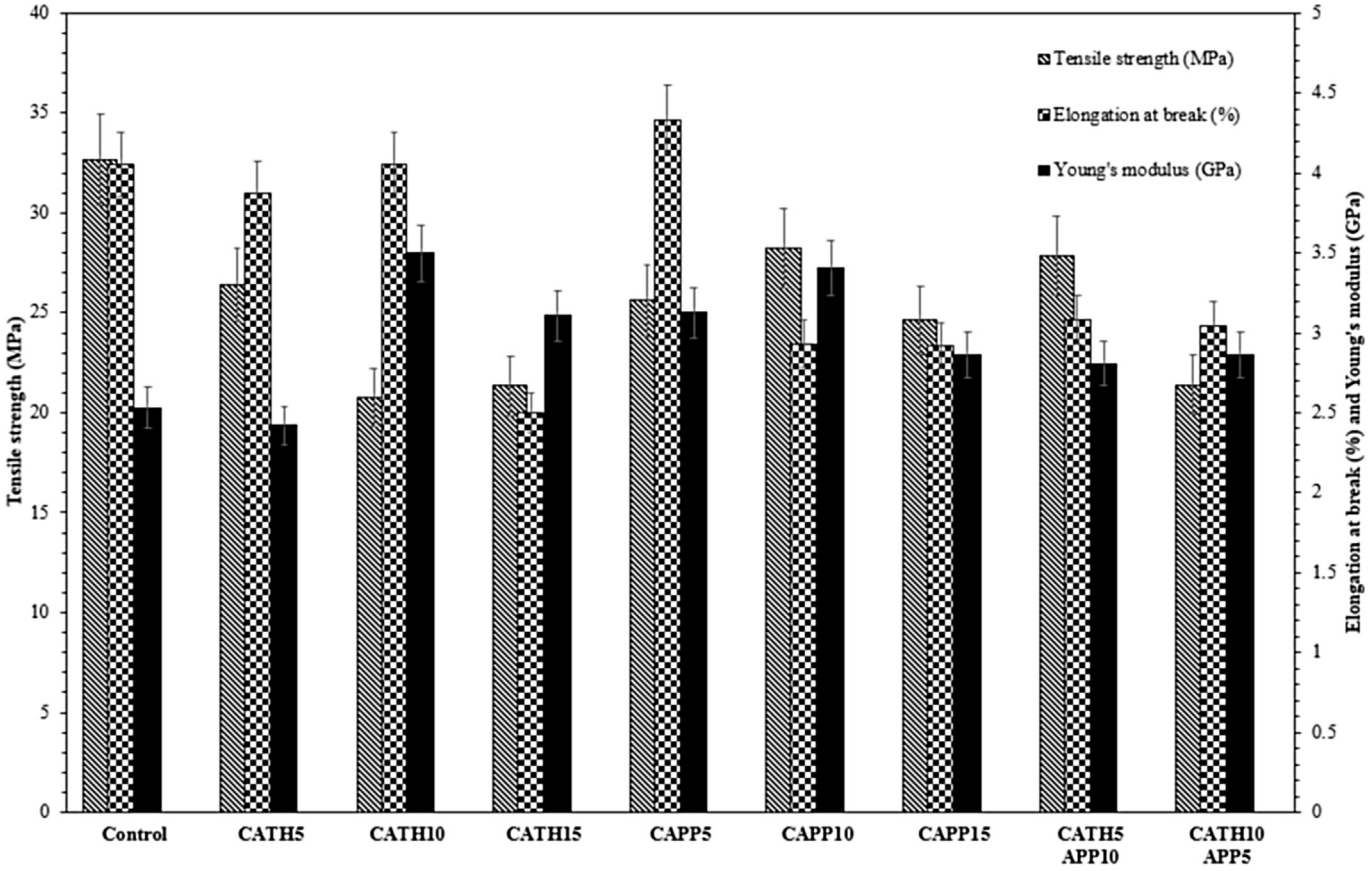

Fig. 8. Tensile strength, Young's modulus and elongation at break of APP and ATH loaded EFB/epoxy composites.

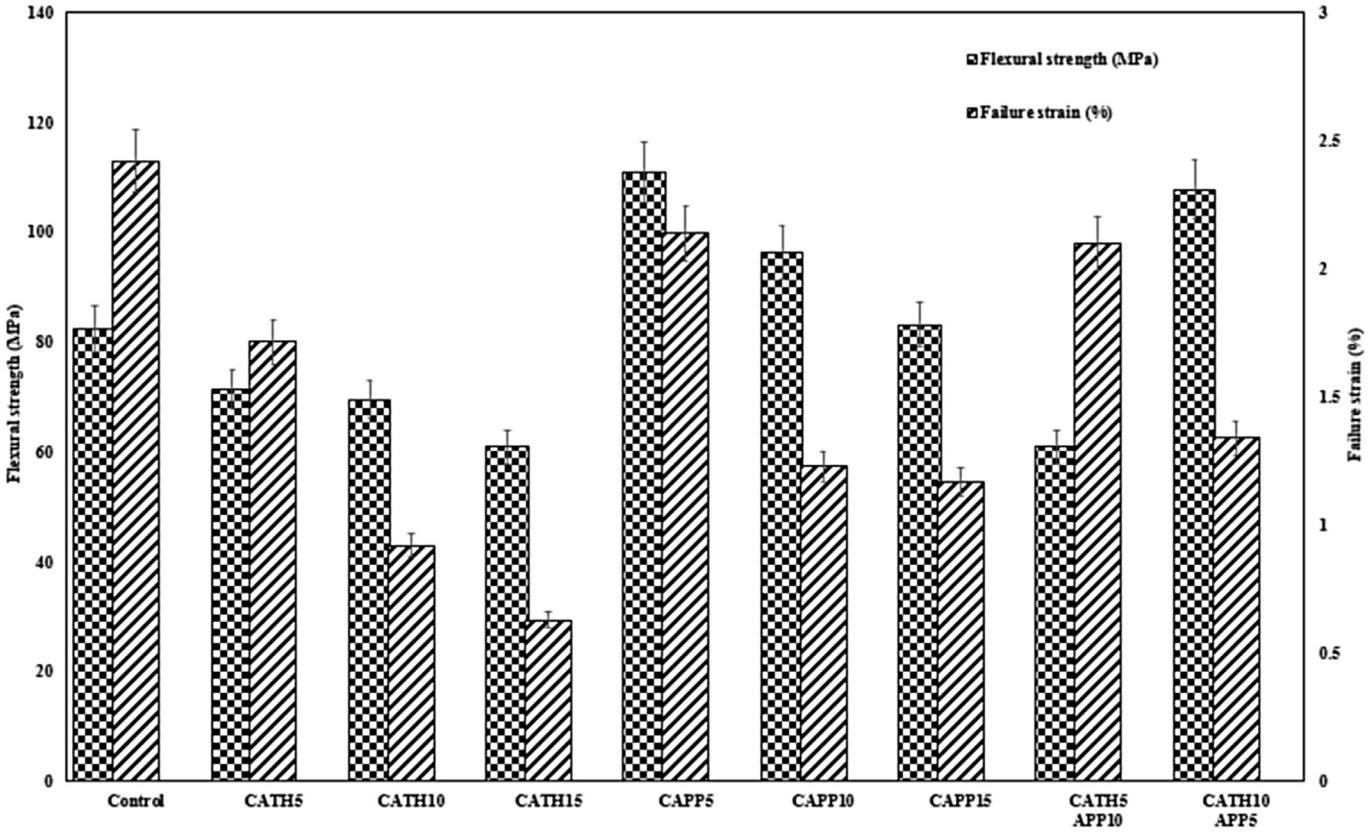

Fig. 9. Flexural properties of ATH and APP filled EFB/epoxy composites.

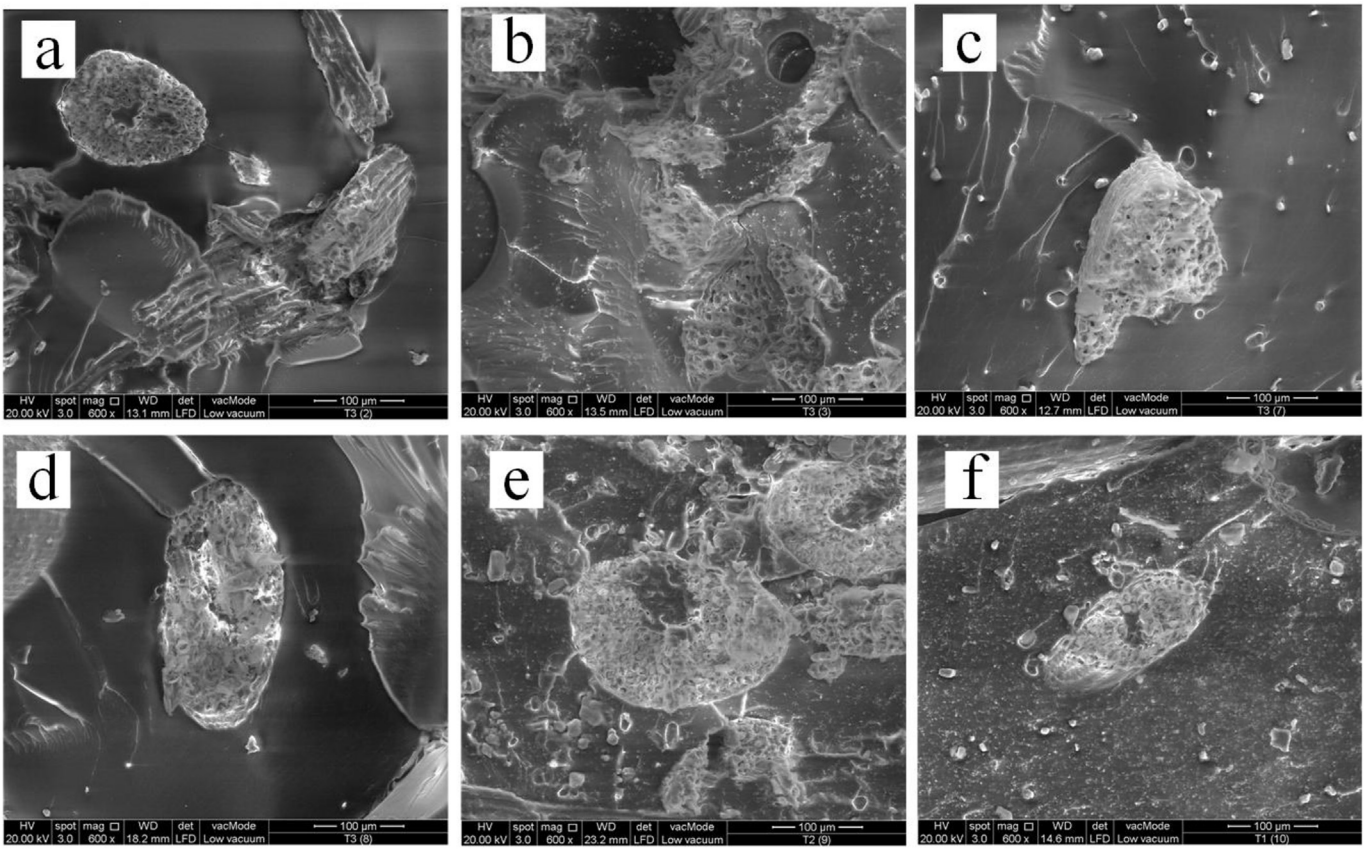

Fig. 10. Morphology of (a) control, (b) CATH5, (c) CAPP10, (d) CAPP15, (e) CATH5APP10 and (f) CATH10APP5 at 600 ×.

3.7. Morphology

The SEM micrographs of tensile fracture surface of the control, 5 wt·% ATH and APP-loaded and ATH/APP hybrid formulations are exhibited in Fig. 10. Homogenous distribution of flame retardants and no obvious void content were observed in the SEM micrographs. The mechanical properties can be affected by the physical characteristics of the polymer, types of additive, additive concentration and filler dimension, distribution and shape. The surface interaction between filler and polymer matrix plays a key factor in the fracture mechanism and crystalline behavior of the polymer, both of which directly influence the mechanical properties of the formulations [42].

No additive is present in the control sample (Fig. 10(a)) whereas the addition of ATH particles (CATH5) is visible as shown in Fig. 10(b). For the composites containing 10 wt·% and 15 wt·% APP contents, the particles can be observed in Fig. 10(c) and (d), respectively. The FR fillers are visible in both CATH5APP10 and CATH10APP5 formulations (Fig. 10(f) and (g)).

4. Conclusions

The effective amount of IFRs required to provide the best flame retardant behaviors of EFB-epoxy based composites was examined. The hybrid of 10 wt·% APP and 5 wt·% ATH was the formulation which could meet the aircraft interior FAR requirements in terms of vertical Bunsen burner test. Other formulations that were investigated failed to meet the Bunsen burner test requirements. It was observed that ATH typically required a greater concentration to create an acceptable FR-based systems, but increasing ATH concentration evidently deteriorates the mechanical characteristics. The incorporation of APP was found to reduce the degradation temperature, however APP depicted the capability of an enhanced charring, as revealed in TGA, ascribed to the formation of NF phosphorylation, zero drip flame time and reduced GH. Introducing FRs, either ATH or APP alone, showed much lower flame retardant behaviors, lower mass residue and higher gross heat of combustion than those of the ATH/APP coupled systems. This depicted the establishment of synergistic effect, which can be attributed to the effect of ATH and APP mixture upon combustion that besides water, forms two different shielding systems including a ceramic metal oxide and aluminum orthophosphate with more complete elimination of ammonia and water in the vapor phase. Generally, the addition of FRs reduced the tensile strength and strain of composites and the incorporation of ATH fillers decreased the flexural strength and strain of composites as compared to those of the control sample.

Acknowledgments

This work was supported in part by the Ministry of Science, Technology and Innovation (MOSTI) Malaysia under Grant 03-02-12-SF0212 as well as the Faculty of Engineering at The University of Nottingham Malaysia Campus.

References

[1] Dorez G, et al. Thermal and fire behavior of natural fibers/PBS biocomposites. Polym Degrad Stab 2013;98(1):87–95.
[2] Yao F, et al. Thermal decomposition kinetics of natural fibers: activation energy with dynamic thermogravimetric analysis. Polym Degrad Stab 2008;93(1):90–8.
[3] Hesser F. Environmental advantage by choice: ex-ante LCA for a new Kraft

pulp fibre reinforced polypropylene composite in comparison to reference materials. Compos Part B Eng 2015;79:197–203.
[4] Scarponi C, Messano M. Comparative evaluation between E-Glass and hemp fiber composites application in rotorcraft interiors. Compos Part B Eng 2015;69:542–9.
[5] Rwawiire S, et al. Development of a biocomposite based on green epoxy polymer and natural cellulose fabric (bark cloth) for automotive instrument panel applications. Compos Part B Eng 2015;81:149–57.
[6] Thakur VK, Thakur MK. Processing and characterization of natural cellulose fibers/thermoset polymer composites. Carbohydr Polym 2014;109(0):102–17.
[7] Anbukarasi K, Kalaiselvam S. Study of effect of fibre volume and dimension on mechanical, thermal, and water absorption behaviour of luffa reinforced epoxy composites. Mater Des 2015;66(Part A):321–30.
[8] Wen P, et al. One-pot synthesis of a novel s-triazine-based hyperbranched charring foaming agent and its enhancement on flame retardancy and water resistance of polypropylene. Polym Degrad Stab 2014;110(0):165–74.
[9] Fox DM, et al. Flame retarded poly(lactic acid) using POSS-modified cellulose. 2. Effects of intumescing flame retardant formulations on polymer degradation and composite physical properties. Polym Degrad Stab 2014;106(0):54–62.
[10] Horacek H, Pieh S. The importance of intumescent systems for fire protection of plastic materials. Polym Int 2000;49(10):1106–14.
[11] Jimenez M, Duquesne S, Bourbigot S. Intumescent fire protective coating: toward a better understanding of their mechanism of action. Thermochim acta 2006;449(1):16–26.
[12] Zhang L, Li J, Ding X. Research of the properties of flame-retardant flexible PVC. Am J Mater Am J Mater Res 2014;1(1):20–5.
[13] Walker, K., A. Isarov, and T. Chen, Fire performance synergies of metal hydroxides and metal molybdates in antimony-free flexible PVC.
[14] Arao Y, et al. Improvement on fire retardancy of wood flour/polypropylene composites using various fire retardants. Polym Degrad Stab 2014;100(0):79–85.
[15] Castrovinci A, et al. Ammonium polyphosphate–aluminum trihydroxide antagonism in fire retarded butadiene–styrene block copolymer. Eur Polym J 2005;41(9):2023–33.
[16] Gallo E, et al. Tailoring the flame retardant and mechanical performances of natural fiber-reinforced biopolymer by multi-component laminate. Compos Part B Eng 2013;44(1):112–9.
[17] Boccarusso, L., et al., Hemp fabric/epoxy composites manufactured by infusion process: improvement of fire properties promoted by Ammonium Polyphosphate. Composites Part B: Engineering.
[18] Lau K-t, Hoi-yan Cheung K, Hui D. Natural fiber composites. Compos Part B Eng 2009;40(7):591–3.
[19] El-Sabbagh A, et al. Processing parameters and characterisation of flax fibre reinforced engineering plastic composites with flame retardant fillers. Compos Part B Eng 2014;62:12–8.
[20] Jeencham R, Suppakarn N, Jarukumjorn K. Effect of flame retardants on flame retardant, mechanical, and thermal properties of sisal fiber/polypropylene composites. Compos Part B Eng 2014;56:249–53.
[21] Chen X, et al. New glass fiber/bismaleimide composites with significantly improved flame retardancy, higher mechanical strength and lower dielectric loss. Compos Part B Eng 2015;71:96–102.
[22] Lee K-Y, et al. Hierarchical composites reinforced with robust short sisal fibre preforms utilising bacterial cellulose as binder. Compos Sci Technol 2012;72(13):1479–86.
[23] Suardana NPG, Ku MS, Lim JK. Effects of diammonium phosphate on the flammability and mechanical properties of bio-composites. Mater Des 2011;32(4):1990–9.
[24] Chapple S, Anandjiwala R. Flammability of natural fiber-reinforced composites and strategies for fire retardancy: a review. J Thermoplast Compos Mater 2010;23(6):871–93.
[25] Marcovich NE, Reboredo MM, Aranguren MI. Modified woodflour as thermoset fillers: II. Thermal degradation of woodflours and composites. Thermochim Acta 2001;372(1–2):45–57.
[26] Yang H, et al. Characteristics of hemicellulose, cellulose and lignin pyrolysis. Fuel 2007;86(12):1781–8.
[27] Reti C, et al. Flammability properties of intumescent PLA including starch and lignin. Polym Adv Technol 2008;19(6):628–35.
[28] Le Bras M, et al. Intumescent polypropylene/flax blends: a preliminary study. Polym Degrad Stab 2005;88(1):80–4.
[29] Gao M, Wu W, Yan Y. Thermal degradation and flame retardancy of epoxy resins containing intumescent flame retardant. J Therm Analysis Calorim 2009;95(2):605–8.
[30] Wu CS, et al. Thermal stability of epoxy resins containing flame retardant components: an evaluation with thermogravimetric analysis. Polym Degrad Stab 2002;78(1):41–8.
[31] Zhang W, et al. The influence of the phosphorus-based flame retardant on the flame retardancy of the epoxy resins. Polym Degrad Stab 2014;109:209–17.
[32] Deng C-L, et al. An intumescent flame retardant polypropylene system with simultaneously improved flame retardancy and water resistance. Polym Degrad Stab 2014;108:97–107.
[33] Shumao L, et al. Influence of ammonium polyphosphate on the flame retardancy and mechanical properties of ramie fiber-reinforced poly(lactic acid) biocomposites. Polym Int 2010;59(2):242–8.
[34] Zhang ZX, et al. Effect of flame retardants on mechanical properties, flammability and foamability of PP/wood–fiber composites. Compos Part B Eng 2012;43(2):150–8.
[35] De Chirico A, et al. Flame retardants for polypropylene based on lignin. Polym Degrad Stab 2003;79(1):139–45.
[36] Patrick Lim WK, et al. Effect of intumescent ammonium polyphosphate (APP) and melamine cyanurate (MC) on the properties of epoxy/glass fiber composites. Compos Part B Eng 2012;43(2):124–8.
[37] Hapuarachchi T, Peijs T. Aluminium trihydroxide in combination with ammonium polyphosphate as flame retardants for unsaturated polyester resin. eXPRESS Polym Lett 2009;3(11):743–51.
[38] Kurt R, MENGELOĞLU F. Utilization of boron compounds as synergists with ammonium polyphosphate for flame retardant wood-polymer composites. Turkish J Agric For 2011;35(2):155–63.
[39] Umemura T, et al. Synergy effects of wood flour and fire retardants in flammability of wood-plastic composites. Energy Procedia 2014;56(0):48–56.
[40] Petersen MR, et al. Mechanical properties of fire-retardant glass fiber-reinforced polymer materials with alumina tri-hydrate filler. Compos Part B Eng 2015;78(0):109–21.
[41] Ramazani SAA, et al. Investigation of flame retardancy and physical–mechanical properties of zinc borate and aluminum hydroxide propylene composites. Mater Des 2008;29(5):1051–6.
[42] Lu M, Zhang S, Yu D. Study on poly(propylene)/ammonium polyphosphate composites modified by ethylene-1-octene copolymer grafted with glycidyl methacrylate. J Appl Polym Sci 2004;93(1):412–9.